

# The great isotopic dichotomy of the early Solar System

Thomas S. Kruijer<sup>1\*</sup>, Thorsten Kleine<sup>2</sup>, Lars E. Borg<sup>1</sup>

<sup>1</sup>Nuclear and Chemical Sciences Division, Lawrence Livermore National Laboratory, 7000 East Avenue (L-231), Livermore, CA 94550, USA

<sup>2</sup>Institut für Planetologie, University of Münster, Wilhelm-Klemm-Straße 10, 48149, Münster, Germany

Revised manuscript submitted as Review Article to *Nature Astronomy*

Version: 27 September 2019

Main text: 4787 words

Abstract: 194 words

5 figures

95 References

\*Corresponding author:

E-mail: [kruijer1@llnl.gov](mailto:kruijer1@llnl.gov)

Phone: +1-925-42-29262

24  
25  
26  
27  
28  
29  
30  
31  
32  
33  
34  
35  
36  
37  
38  
39  
40  
41  
42  
43  
44  
45  
46  
47  
48  
49  
50  
51  
52  
53  
54  
55  
56  
57  
58  
59  
60  
61  
62  
63  
64  
65  
66  
67

**Keywords:**

Meteorites, isotopes, short-lived radionuclides, protoplanetary disk, accretion, planetesimals, Jupiter

**Summary paragraph**

The isotopic composition of meteorites and terrestrial planets holds important clues about the earliest history of the Solar System and the processes of planet formation. Recent work has shown that meteorites exhibit a fundamental isotopic dichotomy between *non-carbonaceous* (NC) and *carbonaceous* (CC) groups, which most likely represent material from the inner and outer Solar System, respectively. Here we review the isotopic evidence for this NC-CC dichotomy, discuss its origin, and highlight the far-reaching implications for the dynamics of the solar protoplanetary disk. The NC-CC dichotomy combined with the chronology of meteorite parent body accretion mandate an early and prolonged spatial separation of inner (NC) and outer (CC) disk reservoirs, lasting between ~1 and ~4 million years (Myr) after Solar System formation. This is most easily reconciled with the early and rapid growth of Jupiter’s core, inhibiting significant exchange of material from inside and outside its orbit. The growth and migration of Jupiter also led to the later implantation of CC bodies into the inner Solar System and, therefore, can explain the co-occurrence of NC and CC bodies in the asteroid belt, and the delivery of volatile- and water-rich CC bodies to the terrestrial planets.

**1. Introduction**

The Solar System formed by the gravitational collapse of a molecular cloud core, which resulted in the formation of a circumsolar disk of gas and dust (sometimes called the ‘solar nebula’). This disk was ultimately transformed into a planetary system consisting of a single central star, the Sun, surrounded by four terrestrial planets in the inner Solar System, four giant planets in the outer Solar System beyond the ‘snow line’, and a multitude of smaller bodies, including asteroids, moons, dwarf planets and comets. To understand how the Solar System evolved towards its present-day configuration, the events and processes occurring during the earliest stages of Solar System history must be reconstructed at a very high temporal and spatial resolution. Although astronomical observations<sup>1</sup> and dynamical modelling<sup>2</sup> provide fundamental insights into the structure and dynamics of protoplanetary disks, and the processes of planetary accretion, the study of meteorites allows reconstructing the Solar System’s earliest history with unprecedented resolution in time and space. Recent analytical advances in the precision of isotope ratio measurements not only make it possible to date meteorites at sub-million-year precision<sup>3-5</sup> (see Box 1), but also to identify distinct nucleosynthetic isotopic signatures. This allows genetic links between planetary materials to be determined and helps constrain the area of the disk a given meteorite originated<sup>6-8</sup>.

Most meteorites derive from asteroids presently located in the main asteroid belt between Mars and Jupiter (at ~2.0-3.3 au), and have traditionally been viewed as samples from bodies that formed where they are found today. However, recently this perspective has changed dramatically with the discovery of a fundamental genetic dichotomy observed in the nucleosynthetic isotope signatures of *non-carbonaceous* (NC) and *carbonaceous* (CC) meteorites<sup>6,8,9</sup>. This discovery, combined with the establishment of a precise chronology for the accretion of meteorite parent bodies, has enabled the integration of meteoritic constraints into large-scale models of disk evolution and planet formation.

## 69 **2. The non-carbonaceous–carbonaceous meteorite dichotomy**

70 Nucleosynthetic isotope anomalies arise from the heterogeneous distribution of presolar phases, and  
 71 ultimately reflect that the Solar System incorporated material from different stellar sources. As evident  
 72 from analyses of presolar grains contained in primitive meteorites, the Solar System’s molecular cloud  
 73 comprised materials with strongly variable isotopic compositions<sup>10</sup>. Although processes within the  
 74 Solar System’s parental molecular cloud and/or the circumsolar disk homogenized these materials  
 75 relatively well, small heterogeneities exist that have been sampled at the scale of meteorite components,  
 76 bulk meteorites, and planets<sup>11</sup>. Nucleosynthetic isotope anomalies have been identified for many  
 77 elements, but here we will focus on those that are most relevant for the definition of the NC-CC  
 78 dichotomy and, hence, provide the most detailed insights into the dynamics of the early Solar System.

79 Meteorites exhibit significant isotope anomalies for elements like O, Cr, and Ti (note that the O isotope  
 80 anomalies are not nucleosynthetic in origin, but nevertheless are indicative of spatial or temporal  
 81 changes of solid material in the disk<sup>12</sup>). As such, it is no surprise that the NC-CC dichotomy was first  
 82 recognized based on isotope anomalies for these three elements<sup>8</sup>. The dichotomy is most clearly  
 83 observed when different isotope anomalies (e.g., <sup>54</sup>Cr vs. <sup>50</sup>Ti) are plotted against each other (Fig. 1). In  
 84 spite of isotope variations among bulk meteorites within each reservoir, there is a clear ‘gap’ between  
 85 the NC and CC reservoirs, indicating that there has not been significant mixing of NC and CC materials  
 86 during the formation of meteorites. Subsequent studies demonstrated that the NC-CC dichotomy  
 87 extends to other elements, such as Ni<sup>13,14</sup> (Fig. 1d) and Mo<sup>6,9,15,16</sup> (Fig. 2a). Molybdenum is especially  
 88 useful in identifying the NC-CC dichotomy because it allows anomalies of distinct origins to be  
 89 distinguished and because, unlike Ti and Cr, the isotopic composition of Mo can be analysed in  
 90 essentially all meteorites. Specifically, the heterogeneous distribution of carriers enriched in nuclides  
 91 produced in the slow neutron capture process (*s*-process) of stellar nucleosynthesis and the rapid  
 92 neutron capture process (*r*-process) results in different patterns of Mo isotope anomalies within  
 93 individual samples<sup>17</sup>. These variable nucleosynthetic components are most clearly seen in a plot of  
 94  $\epsilon^{95}\text{Mo}$  versus  $\epsilon^{94}\text{Mo}$  (the parts-per-10,000 deviations of the <sup>95</sup>Mo/<sup>96</sup>Mo and <sup>94</sup>Mo/<sup>96</sup>Mo ratios from  
 95 terrestrial standard values), where NC and CC meteorites define two separate and parallel *s*-process  
 96 mixing lines with a resolved offset between the two lines (Fig. 2a). This offset reflects an approximately  
 97 homogeneous enrichment in *r*-process (and possibly *p*-process<sup>15,16</sup>) nuclides in the CC over the NC  
 98 reservoir<sup>6,18</sup>. The fact that Mo can be analysed in a wide range of sample types leads to the realization  
 99 that the NC-CC dichotomy is a fundamental and ubiquitous characteristic of the entire meteorite record.

100 As will be discussed in more detail below, the NC-CC dichotomy most likely reflects the separation of  
 101 the early Solar System into an inner and outer disk separated by Jupiter. As carbonaceous chondrites  
 102 are commonly assumed to have accreted at greater heliocentric distances than ordinary and enstatite  
 103 chondrites, and because the Earth and Mars plot within the NC field (Fig. 1), the NC reservoir represents  
 104 the inner and the CC reservoir the outer Solar System<sup>8</sup> (Fig. 5).

105

## 106 **3. Meteorite chronology in light of the NC-CC dichotomy**

107 Utilizing the NC-CC dichotomy of meteorites to understand the evolution of the early Solar System and  
 108 determining whether the dichotomy reflects temporal and/or spatial changes in the isotopic composition  
 109 of the disk, requires knowledge of the timescales of meteorite parent body accretion. However, parent  
 110 body accretion cannot be dated directly, but must be inferred either by dating the formation of a specific

111 component (e.g., chondrules) that is closely linked in time to the accretion of their parent body, or  
112 alternatively, by dating a specific chemical differentiation process (e.g., core formation), which can be  
113 linked to the time of parent body accretion via thermal modelling. Rather than providing a  
114 comprehensive summary of the chronology of meteorites, we will here focus on those ages that provide  
115 the most precise constraints on the accretion timescales of NC and CC meteorite parent bodies. Below  
116 we distinguish between the accretion ages for the parent bodies of differentiated meteorites (Section  
117 3.1) and of chondrite parent bodies (Section 3.2). Note that all ages are given relative to the start of  
118 Solar System history  $4567.2 \pm 0.2$  million years (Myr) ago<sup>3,19</sup> as defined by the ages of Ca-Al-rich  
119 inclusions (CAIs; see Box 1).

### 120 **3.1. Differentiated meteorites and the first planetesimals**

121 Differentiated meteorites include samples from the metallic cores (i.e., iron meteorites) as well as  
122 silicate mantles and crusts (e.g., Angrites, eucrites, ureilites) of differentiated asteroids. Collectively the  
123 meteorite ages demonstrate that planetesimal differentiation occurred within the first few million years  
124 after CAI formation<sup>20</sup> (Myr), consistent with heating driven mainly by <sup>26</sup>Al decay<sup>21</sup>. The most direct  
125 evidence for early planetesimal differentiation comes from the Hf-W chronometry of 'magmatic' iron  
126 meteorites, which are thought to sample the cores of differentiated protoplanets<sup>22</sup>. The Hf-W model  
127 ages of core formation (Box 1) are between ~0.3 and ~1.8 Myr for NC irons, and between ~2.2 and  
128 ~2.8 Myr for CC irons<sup>4,9</sup> (Fig. 3b). Combining the Hf-W ages with thermal modelling of bodies  
129 internally heated by <sup>26</sup>Al decay demonstrates that NC iron meteorite parent bodies accreted less than  
130 0.5 Myr, whereas CC iron meteorite parent bodies accreted less than 1 Myr after CAI formation<sup>4,9</sup> (Fig.  
131 4). Iron meteorite parent bodies, therefore, are among the first planetesimals formed in the Solar System.  
132 A corollary of this observation is that rapid formation of differentiated planetesimals (i.e. of iron  
133 meteorite parent bodies) was possible not only in the inner-most terrestrial planet region<sup>23</sup>, but also in  
134 the outer disk (i.e., the CC reservoir).

135 Accretion timescales can in principle also be inferred for the parent bodies of differentiated achondrites  
136 (e.g., Angrites, eucrites, ureilites). However, these accretion ages are less well constrained, because there  
137 are additional parent-to-daughter (e.g., Hf-W or Al-Mg) fractionation events in the silicate mantles  
138 subsequent to core formation. The isotopic compositions of these samples, therefore, reflect more than  
139 one differentiation event, making the model ages for core formation more uncertain. Nevertheless, there  
140 is general agreement that the angrite and eucrite parent bodies accreted well within the first ~1–2 Myr  
141 of the Solar system<sup>24-26</sup>, and thus as early as the iron meteorite parent bodies. However, extremely early  
142 accretion ages reported for the angrite and ureilite parent bodies<sup>27,28</sup> hinge on the contested<sup>29,30</sup>  
143 assumption of a heterogeneous distribution of <sup>26</sup>Al in the Solar System, and the ureilite parent body in  
144 particular may have accreted slightly later than the parent bodies of other differentiated objects<sup>31</sup>.  
145 Regardless of these uncertainties, the chronology of differentiated achondrites indicates that these  
146 meteorites, like the irons, derive from an early generation of planetesimals.

147

### 148 **3.2. 'Late' accretion of chondrite parent bodies**

149 Chondrites are thought to derive from asteroids that never melted and, therefore, preserved components  
150 that formed prior to their accretion. Of these, millimetre-sized igneous spherules known as chondrules  
151 are not only the most dominant, but also the most extensively dated component. Different mechanisms  
152 for chondrule formation have been proposed, but no consensus about their formation process has yet  
153 been reached<sup>32</sup>. Chondrules may have formed by melting of dust aggregates in the solar protoplanetary  
154 disk, which might have facilitated the accumulation of dust into planetesimals<sup>33,34</sup>. They may also have

155 formed during protoplanetary impacts and would then merely be a by-product of planet formation<sup>35</sup>.  
156 Regardless of their exact formation process, chondrules formed prior to their assembly into chondrite  
157 parent bodies, and so dating chondrule formation constrains the timescale of chondrite parent body  
158 accretion.

159 Ages for chondrules are typically obtained either by pooling multiple chondrules (Pb-Pb, Hf-W) or by  
160 dating single chondrules (Al-Mg, Pb-Pb). Perhaps the most stringent constraint comes from Al-Mg  
161 chronometry of individual chondrules from the least altered chondrites, revealing clear age peaks at ~2-  
162 3 Myr (for chondrules from ordinary, CV, and CO chondrites) and at ~3.7 Myr (CR chondrites), after  
163 CAI formation<sup>5,36-39</sup> (Fig. 3a). These ages are in excellent agreement with Hf-W<sup>29,34</sup> and Pb-Pb<sup>40-43</sup> ages  
164 of pooled chondrule separates from CV and CR chondrites, indicating that the vast majority of  
165 chondrules formed between ~2 and ~4 Myr after CAI formation (Fig. 3a). Moreover, chondrules from  
166 a given chondrite group formed in a narrow time span of <1 Myr, suggesting they rapidly accreted into  
167 their parent bodies. The youngest chondrule ages of ~4–5 Myr are obtained for CB chondrites<sup>44,45</sup>, but  
168 their formation process likely was different from that of other, more common chondrules<sup>45,46</sup>.

169 Given this consistent picture of chondrule chronology it is surprising that Pb-Pb ages for some  
170 *individual* chondrules from a given chondrite group display a spread in ages from ~0–4 Myr, whereas  
171 Al-Mg ages remain relatively constant<sup>3,47,48</sup>. One possibility to account for the disparity between Pb-Pb  
172 and Al-Mg ages for single chondrules is that <sup>26</sup>Al was heterogeneously distributed among the chondrule  
173 precursors, and that variations in <sup>26</sup>Al abundances, therefore, have no chronological meaning<sup>47,48</sup>. This,  
174 however, is not easily reconciled with the good agreement of Hf-W and Al-Mg ages for meteorites<sup>29,30</sup>,  
175 and with the good agreement between Al-Mg, Hf-W *and* Pb-Pb ages for pooled chondrule separates  
176 (Fig. 3a). A heterogeneous <sup>26</sup>Al distribution would also lead to an apparent range in Al-Mg chondrule  
177 ages, instead of a single well-defined age peak observed for each chondrule group. It should be noted  
178 that chondrules for which individual Pb-Pb ages have been reported are exceptionally large<sup>47</sup> and may,  
179 therefore, be unrepresentative of the broader chondrule population. The Pb-Pb ages may also be shifted  
180 towards older ages due to loss of short-lived <sup>222</sup>Rn in the <sup>238</sup>U-<sup>206</sup>Pb decay chain<sup>5</sup>. Thus, in spite of the  
181 ancient Pb-Pb ages reported for a few chondrules, there is little doubt that the vast majority of  
182 chondrules formed between ~2 and ~4 Myr after CAI formation.

183 Besides estimates based on chondrule ages, the accretion times of chondrite parent bodies have also  
184 been determined using thermal modelling of asteroids heated internally by <sup>26</sup>Al decay, combined with  
185 either the inferred peak metamorphic temperatures reached inside these bodies<sup>49</sup> or with the chronology  
186 of alteration products (e.g., carbonates and secondary fayalites)<sup>50-52</sup>. Using these approaches generally  
187 results in accretion ages that are consistent with the isotopic ages of chondrules. For instance, for the  
188 CV chondrite parent body the 2.5–3.3 Myr accretion age obtained from thermal modeling<sup>50,51</sup> is in good  
189 agreement with the aforementioned CV chondrule ages of 2–3 Myr after CAI formation. For CM  
190 chondrites, for which no chondrule ages are available, a 3.0–3.5 Myr accretion age is obtained<sup>52</sup>,  
191 suggesting that this body formed somewhat later than the ordinary, CV, and CO chondrite parent bodies  
192 (Fig. 3a).

193 In summary, the chronology of chondrules and secondary alteration products in primitive chondrites,  
194 as well as thermal modelling of bodies heated by <sup>26</sup>Al decay, indicate that chondrite parent body  
195 accretion occurred between ~2 and ~4 Myr after CAI formation, and post-dated the accretion of  
196 differentiated asteroids. In the NC reservoir, meteorite parent body accretion ceased at ~2 Myr, when  
197 the ordinary chondrite parent bodies formed, but in the CC reservoir continued until at least ~3–4 Myr,  
198 when the CR and CM chondrite parent bodies formed (Fig. 4).

199

## 200 **4. Dynamical implications of the NC-CC dichotomy**

201 Linking the chronology of meteorite parent body accretion with the NC-CC dichotomy provides  
202 fundamentally new insights into the dynamics and large-scale structure of the solar protoplanetary disk,  
203 the formation and growth history of Jupiter, and the accretion dynamics of terrestrial planets, including  
204 the delivery of water and highly volatile species to Earth.

### 205 **4.1. Origin of the dichotomy and structure of the solar protoplanetary disk**

206 To understand the origin of the NC-CC dichotomy, it is useful to summarize its three key characteristics.  
207 First, the dichotomy requires a larger fraction of nuclides produced in neutron-rich stellar environments  
208 to be present in the CC reservoir compared to the NC reservoir. This is manifest by enrichments in  $^{50}\text{Ti}$ ,  
209  $^{54}\text{Cr}$ , and *r*-process Mo isotopes in CC materials relative to NC materials. Second, the same isotopic  
210 characteristics, but with more pronounced enrichments, are typically also found in 'normal' CAIs<sup>11,53</sup>,  
211 which are known to have formed very early<sup>3,41,54,55</sup>. Finally, the dichotomy exists for both refractory  
212 (e.g., Ti, Mo) and non-refractory elements (e.g., Cr, Ni), which were likely hosted in distinct carriers.  
213 Based on these observations two scenarios for the origin of the dichotomy can be ruled out. First, the  
214 dichotomy cannot reflect preferential destruction and volatilization of isotopically anomalous material  
215 from thermally labile presolar carriers by locally elevated temperatures within the disk, because such  
216 'thermal processing' would have likely resulted in disparate effects on carriers of elements with  
217 different volatilities. Moreover, there is no *a priori* reason why thermal processing would solely affect  
218 carriers from specific neutron-rich stellar environments, and not also other carrier phases. Second, the  
219 dichotomy also cannot solely result from admixing of isotopically anomalous CAIs to the CC reservoir,  
220 because CAIs contain too little Cr and Ni to have a significant effect on the isotopic composition of  
221 these elements throughout the outer disk<sup>13,56</sup>.

222 Instead, the key characteristics of the dichotomy outlined above are more readily explained if the  
223 isotopic difference between the NC and CC reservoirs is inherited from the Solar System's parental  
224 molecular cloud and was imparted onto the protoplanetary disk during infall from the collapsing  
225 protostellar envelope (Fig. 5). For instance, in a model proposed by Nanne et al.<sup>13</sup> and Burkhardt et al.  
226<sup>56</sup> the isotopic composition of early-infalling material is characterized by enrichments in nuclides from  
227 neutron-rich stellar environments and is similar to that recorded in CAIs, which formed close to the Sun  
228 and were subsequently transported outwards by rapid viscous spreading of the disk<sup>57-59</sup>. This earliest  
229 disk would not only have contained CAIs but also other, less refractory, dust particles<sup>56</sup>. Later infalling  
230 NC material was depleted in nuclides from neutron-rich stellar environments, and provided most of the  
231 mass of the inner disk<sup>59</sup>. The model assumes that the outer disk, which had formed by viscous spreading  
232 of early infalling material, extended beyond the radius at which the later infalling material is added  
233 (Fig. 5). In this case, a signature of the earliest disk would be preserved, in diluted form, as the  
234 composition of the CC reservoir, which is intermediate between those of early- (i.e., CAI-like) and late-  
235 infalling (i.e., NC-like) material. The strength of this model is that it readily accounts for the formation  
236 of CAIs close to the Sun, their subsequent outward transport, and the isotopic link between CAIs and  
237 the CC reservoir by the same process, namely the rapid radial expansion of early-infalling material<sup>13</sup>.  
238 Finally, an origin of the NC-CC dichotomy during later infall implies that the Solar System's parental  
239 molecular cloud was isotopically heterogeneous. It is important to recognize that the magnitude of this  
240 isotopic heterogeneity is on the order of only  $\sim 0.1\%$ . Such extremely small heterogeneities are not  
241 improbable in the large and dynamic structures of molecular clouds.

242

## 243 4.2. The Jupiter barrier

244 Linking the NC-CC dichotomy (Section 2) with the chronology of meteorite parent body accretion  
245 (Section 3) provides key constraints on the formation and growth history of Jupiter. In particular, the  
246 chronology of meteorites demonstrates that meteorite parent body accretion in the NC and CC  
247 reservoirs commenced very early and continued concurrently for several Myr in both reservoirs<sup>9</sup> (Fig.  
248 4). Importantly, the characteristic Mo isotope signatures of the NC and CC reservoirs did not change  
249 significantly during this period, as is evident from the observation that in each reservoir early-formed  
250 iron meteorites and later-formed chondrites plot on single *s*-process mixing lines (i.e., the NC- and CC-  
251 lines; Fig. 2a). The data allow for some deviations from each line, which may reflect small variations  
252 in the characteristic *r*-process signatures of the NC and CC reservoirs, but these differences are small  
253 compared to the overall offset between the NC- and CC-lines. Combined, these data indicate that the  
254 NC and CC reservoirs co-existed, and maintained their isotopic differences, for several Myr<sup>9</sup>.

255 As is evident from the Hf-W ages for iron meteorites, planetesimal accretion in both the NC and CC  
256 reservoirs commenced very early. Consequently, one way to explain the characteristic NC-CC isotopic  
257 difference sampled by these objects is that it reflects the rapid accretion of dust into planetesimals with  
258 more stable orbits, hampering any further mixing of dust from the NC and CC reservoirs. However, this  
259 explanation cannot account for the observation that planetesimals with the same characteristic NC-CC  
260 isotopic difference (i.e., the chondrite parent bodies in both reservoirs; Fig. 4) continued to accrete for  
261 several Myr, because the rapid radial transport of dust in the disk<sup>60,61</sup> would have homogenized the NC-  
262 CC isotopic difference on a much shorter timescale. The prolonged spatial separation of the NC and  
263 CC reservoirs, therefore, requires a barrier against radial transport of material. The most likely candidate  
264 for this barrier is the formation of Jupiter<sup>21</sup>, which would have inhibited the inward drift of most dust  
265 particles<sup>62,63</sup>, preserving the distinct isotopic compositions of the NC and CC reservoirs. By blocking  
266 the sunward drift of dust, the Jupiter barrier also led to a mass-deficient inner Solar System, ultimately  
267 resulting in the Solar System's bimodal structure of four smaller terrestrial planets surrounded by four  
268 gas giant planets<sup>63</sup>.

269 In detail, the efficiency of the Jupiter barrier depends on the grain size of the dust drifting inwards, and  
270 on the size (and hence growth history) of Jupiter. For instance, the Jupiter barrier may have resulted in  
271 a strong filtering effect, whereby small dust grains could still pass through, whereas the drift of larger  
272 grains was efficiently prohibited<sup>64</sup>. While this process may have resulted in small isotopic changes  
273 within the NC reservoir, it evidently did not lead to significant departures of meteorite compositions  
274 from the NC-line<sup>18</sup>, either because the inward drifting CC dust was not accreted efficiently by NC parent  
275 bodies<sup>65</sup> or because the total mass of this material was not sufficient to significantly change the  
276 composition of the inner disk<sup>9,18</sup>.

277 Jupiter not only provides the necessary barrier for separating the NC and CC reservoirs, its growth<sup>66</sup>  
278 and/or migration<sup>67</sup> also provides a mechanism for the inward scattering of CC bodies into the inner  
279 Solar System. This accounts for the co-occurrence of both types of bodies in the present-day asteroid  
280 belt, implying that the compositional diversity of main belt asteroids reflects their formation over a  
281 wide range of heliocentric distances. Further, the inward scattering of objects from beyond Jupiter's  
282 orbit also provides a mechanism for the delivery of CC bodies to the growing terrestrial planets<sup>66</sup>.

283

## 284 4.3. Growth history of Jupiter

285 The standard model for the formation of Jupiter is the core accretion model<sup>68</sup>, in which Jupiter's gaseous  
286 envelope is accreted onto a 'solid' core of 10-20 Earth's masses ( $M_{\oplus}$ ). Once Jupiter's core reached  $\sim 20$

287  $M_{\oplus}$  it significantly hampered the inward drift of dust grains<sup>62</sup>, and when Jupiter reached  $\sim 50 M_{\oplus}$  it  
288 opened a gap in the disk<sup>69</sup>, ultimately leading to inward migration<sup>67</sup> of Jupiter and gravitational  
289 scattering<sup>66</sup> of bodies from beyond its orbit into the inner Solar System (Fig. 5). Within the framework  
290 of this model for Jupiter's formation, and under the assumption that the growth of Jupiter is responsible  
291 for the *initial* separation of the NC and CC reservoirs, the timescale of its growth can be estimated from  
292 the chronology of meteorite parent body accretion within the NC and CC reservoirs.

293 The tightest constraint on the timescale of Jupiter's growth is provided by the early accretion times of  
294 NC and CC iron meteorite parent bodies. As the characteristic *r*-process Mo isotopic difference between  
295 the NC and CC reservoirs did not change significantly after the first planetesimals (i.e., the iron  
296 meteorite parent bodies) had formed in each reservoir, Jupiter's core was likely grown to near its final  
297 size by the time the oldest NC planetesimals formed, at  $<0.5$  Myr after CAI formation<sup>9</sup>. Such a rapid  
298 accretion of Jupiter's core probably requires formation by pebble accretion<sup>68,70,71</sup>.

299 Constraining Jupiter's subsequent growth history is more difficult. In the simplest case, the accretion  
300 ages of NC and CC meteorites reflect the period of time over which no mixing between both reservoirs  
301 occurred<sup>9</sup>. In this case, dynamical mixing of NC and CC bodies could have only occurred after  
302 formation of the youngest CC bodies<sup>9</sup> at  $\sim 3.7$  Myr after CAI formation<sup>29</sup>. In detail, however, the effect  
303 of Jupiter's growth on the composition of the NC and CC reservoirs was likely more complicated. For  
304 instance, accretion of CC bodies may still have occurred while Jupiter already scattered earlier-formed  
305 CC bodies into the inner Solar System, and so Jupiter may have reached  $\sim 50 M_{\oplus}$  earlier than  $\sim 3.7$  Myr  
306 after CAI formation. For instance, within the framework of the Grand Tack model<sup>67</sup>, Jupiter's migration  
307 through the asteroid belt would have terminated planetesimal formation there, so in this case Jupiter  
308 would have likely reached a mass of  $\sim 50 M_{\oplus}$  by  $\sim 2$  Myr, the accretion age of the youngest NC meteorites  
309 (the ordinary chondrites). However, if Jupiter never migrated through the asteroid belt, then  
310 planetesimal formation in the NC reservoir may have also terminated through the depletion of gas  
311 inwards of Jupiter or because most of the dust had already been locked up in planetesimals.  
312 Nevertheless, so far there is no observational evidence suggesting inward scattering of CC bodies during  
313 the time of NC meteorite parent body accretion, and so it seems unlikely that Jupiter reached  $\sim 50 M_{\oplus}$   
314 before  $\sim 2$  Myr. Note that the earliest observed influx of CC bodies into the inner Solar System is at  $\sim 4$   
315 Myr, as recorded in the H isotopic composition of eucrites and Angrites<sup>72,73</sup>. Consistent with this,  
316 Angrites dated at  $\sim 4$ – $5$  Myr after CAI formation<sup>25,74</sup> record the absence of a nebular magnetic field<sup>75</sup>,  
317 indicating that by this time the nebular gas had dissipated. As Jupiter can only grow to its final size of  
318  $\sim 318 M_{\oplus}$  in the presence of nebular gas, Jupiter's accretion must have been completed by this time<sup>75</sup>.  
319 Taking all these observations together suggests that Jupiter's core of  $10$ – $20 M_{\oplus}$  accreted within  $<0.5$   
320 Myr, while Jupiter reached  $\sim 50 M_{\oplus}$  after  $\sim 2$  Myr, and its final size of  $\sim 318 M_{\oplus}$  before  $\sim 4$ – $5$  Myr. This  
321 timescale of Jupiter's accretion is consistent with predictions of the core accretion model<sup>168,76</sup>.

322

#### 323 4.4. Accretion of Earth

324 The NC-CC dichotomy provides a powerful tool to test different terrestrial planet accretion scenarios,  
325 which primarily differ in terms of the extent of radial mixing and the provenance of accreted material<sup>77</sup>.  
326 Of particular interest is the amount of CC material accreted by Earth (and other terrestrial planets),  
327 because this material derives from the most distant sources and therefore provides the tightest  
328 constraints on the extent of radial mixing during terrestrial planet formation. However, for most  
329 elements the inferred amount of CC material in Earth is uncertain, because, owing to isotopic variations  
330 within the NC reservoir (Fig. 1), it depends on the assumed endmember isotopic compositions of Earth's  
331 building material<sup>8</sup>. This situation is different for Mo isotopes, because the amount of CC material



332 accreted by Earth can be determined from the position of Earth's primitive mantle (or bulk silicate  
333 Earth, BSE) among the NC- and CC-lines, irrespective of the position of Earth's building material on  
334 these lines<sup>18</sup>. That the BSE plots between the NC- and CC-lines (Fig. 2b), therefore, indicates that 30–  
335 60% of the BSE's Mo derives from the CC reservoir<sup>18</sup>. As a siderophile (metal-loving) element, the Mo  
336 in the BSE predominantly derives from the last 10–20% of accretion, because the Mo from earlier stages  
337 has been largely removed into Earth's core<sup>78</sup>. Thus, while these data provide no information on whether  
338 Earth accreted CC material during earlier stages, they demonstrate that Earth accreted substantial  
339 amounts of CC material late in its growth history.

340 The last 10–20% of Earth's accretion were strongly influenced by the giant impact that led to the  
341 formation of the Moon<sup>79</sup>, and by the late veneer; the material added to Earth's mantle after this impact.  
342 Budde et al.<sup>18</sup> have shown that the BSE's Mo isotopic composition is best reproduced by either a CC  
343 composition of the Moon-forming impactor, or by mixed NC-CC compositions for the impactor and  
344 the late veneer. In both cases, the Moon-forming impactor contributed CC material to Earth, implying  
345 that this body either was a CC embryo from the outer Solar System, or that it accreted substantial  
346 amounts of CC material itself prior to collision with Earth. Either way, the late accretion of CC material  
347 to Earth likely also delivered water and highly volatile species to Earth<sup>80,81</sup>, suggesting that Earth's  
348 habitability is strongly linked to the very late stages of its formation.

349

## 350 **5. Open questions and future steps**

351 The discovery of the NC-CC isotopic dichotomy has dramatically changed the way by which meteorites  
352 are used for constraining the dynamical evolution of the early Solar System and the nature of planet  
353 formation. Despite this success, several important questions remain. The efficiency of the Jupiter barrier  
354 for separating the NC and CC reservoirs should be better understood, and the isotopic evolution, if any,  
355 of the NC reservoir resulting from the potential inward drift of CC dust remains to be quantified, both  
356 in terms of spatial heterogeneity and temporal evolution. A related question is whether the inferred  
357 rapid formation of Jupiter's core by pebble accretion is compatible with the limited influx of material  
358 from the outer into the inner disk mandated by the preservation of an NC-CC isotopic difference.

359 Another important future step will be to combine the isotopic evidence for the provenance of accreted  
360 material derived from the NC-CC dichotomy with dynamical models of terrestrial planet formation. For  
361 instance, a scenario linking the late accretion of outer Solar System material by the Earth to an orbital  
362 instability of the gas giant planets around the time of the Moon-forming impact<sup>18,82</sup> remains to be tested.  
363 It will also be important to combine the isotopic and dynamical constraints with the known chronology  
364 of terrestrial planet formation. For instance, Schiller et al.<sup>65</sup> proposed that Earth accreted a large fraction  
365 (~40%) of CC-derived dust from the outer Solar System very early, within the lifetime of the  
366 protoplanetary disk (i.e., within ~5 Myr after CAI formation). One implication of this model is that  
367 about half of the Earth's mass was accreted by this time. However, the <sup>182</sup>Hf-<sup>182</sup>W chronology of core  
368 formation on Earth indicates that such a rapid accretion is only possible for a very high degree of core-  
369 mantle re-equilibration during each impact, including the Moon-forming event<sup>83-85</sup>. It is unknown,  
370 however, if such high degrees of equilibration have been achieved<sup>86</sup>.

371 Finally, Mars will play a key role in addressing some of these issues, because it likely accreted within  
372 the first 10 Myr of the Solar System<sup>87,88</sup>. As such, Mars may have recorded the inward scattering of CC  
373 bodies during Jupiter's growth and/or migration but may have also accreted CC-derived dust that passed  
374 through the Jupiter barrier. However, the nature, timing, and magnitude of the addition of CC material

375 to Mars has yet to be investigated<sup>89</sup>. Clearly, addressing all these questions will lead to major advances  
376 in understanding the early Solar System and the fundamental process of planet formation.

377

378

379 **Box. 1: Dating meteorites using isotope chronometers.**

380 Radioactive decay systems used for dating meteorites can be subdivided into long-lived and short-lived  
381 chronometers. Of these, the <sup>207</sup>Pb-<sup>206</sup>Pb isotope systems, which is based on the decay of long-lived <sup>235</sup>U  
382 and <sup>238</sup>U, can provide very precise absolute ages for meteorites and their components<sup>3,19,74</sup>, as long as  
383 they are corrected for variable <sup>235</sup>U/<sup>238</sup>U in early Solar System materials<sup>90</sup>. Short-lived radionuclides are  
384 isotopes that existed at the beginning of Solar System history but that have since decayed. Hence, their  
385 presence in the early Solar System can only be detected by studying the isotopic composition of their  
386 daughter isotopes. Important examples of short-lived chronometers that are highly relevant for early  
387 solar system chronology include the <sup>26</sup>Al-<sup>26</sup>Mg (half-life: ~0.7 Myr) and <sup>182</sup>Hf-<sup>182</sup>W (half-life: ~9 Myr)  
388 systems.

389 For establishing a precise chronology of the early Solar System, it is useful to define a common  
390 reference point, which is typically defined by the formation of the oldest dated solids, known as Ca-Al-  
391 rich inclusions (CAIs). These refractory inclusions are thought to have formed close the young Sun<sup>91</sup>,  
392 and were subsequently transported outwards to the accretion region of carbonaceous chondrites<sup>57,58</sup>.  
393 The Pb-Pb age of CAIs of 4567.2±0.2 Myr is generally considered to effectively date the start of Solar  
394 System history, or 'time-zero' in cosmochemistry<sup>3,19</sup>. CAIs also have the highest initial <sup>26</sup>Al/<sup>27</sup>Al and  
395 <sup>182</sup>Hf/<sup>180</sup>Hf ratios of any meteoritic material<sup>30,54,55,92</sup>, making them pivotal reference points for the Solar  
396 System's initial compositions of various decay systems. However, there are also CAIs that lack evidence  
397 for live <sup>26</sup>Al, and these CAIs are thought to have formed slightly earlier than the more common 'normal'  
398 CAIs, prior to injection of <sup>26</sup>Al into the Solar System<sup>93-95</sup>. Nevertheless, in early Solar System  
399 chronology, ages are generally given as the time elapsed since formation of 'normal' CAIs dated at  
400 4567.2±0.2 Myr.

401 The Al-Mg system provides very precise relative isochron ages for meteorite components such as  
402 CAIs<sup>54,55</sup> and chondrules<sup>5,36,38</sup>. These ages are chronologically meaningful only when <sup>26</sup>Al was  
403 distributed homogeneously throughout the solar system, which is debated<sup>27-30</sup>.

404 The Hf-W system is widely used to date planetary core formation, both on meteorite parent bodies and  
405 on larger bodies like the Earth<sup>83,84</sup>. This is because both Hf and W are refractory elements but have  
406 different geochemical affinities during metal-silicate separation. As W is moderately siderophile and  
407 Hf strongly lithophile, core-mantle differentiation results in high Hf/W in the mantle, and Hf/W of  
408 essentially zero in the core. Hence, the Hf-W system can be used to provide model ages for the timing  
409 of core formation in planetary bodies that accreted during the earliest stages of Solar System history  
410 (i.e., within the effective lifetime of <sup>182</sup>Hf).

411

412 Correspondence should be addressed to T.S.K.

413

414 **Acknowledgements:** We are especially grateful to G. Budde and C. Burkhardt for many discussions  
415 about the NC-CC dichotomy, and for the collaborative effort that led to the identification of the  
416 dichotomy and for the development of some of the ideas presented in this article. We thank G.  
417 Brennecka, J. Cuzzi, A. Morbidelli, F. Nimmo, and E.A. Worsham for discussions, and the reviewers

418 and editor for constructive comments. This study was performed under the auspices of the US DOE by  
419 Lawrence Livermore National Laboratory under Contract DE-AC52-07NA2734. Funding from the  
420 Laboratory Directed Research and Development Program at Lawrence Livermore National Laboratory  
421 (Grants: 17-ERD-001 to L.E.B. and 20-ERD-001 to T.S.K.), from the European Research Council  
422 (ERC Consolidator Grant no. 616564 'ISOCORE' to T.K.) and from the Deutsche  
423 Forschungsgemeinschaft as part of the Collaborative Research Center TRR 170 (subproject B3) is  
424 gratefully acknowledged. This is TRR publication no. 81.

425

## 426 **References**

- 427 1 Brogan, C. L. *et al.* The 2014 ALMA long baseline campaign: First results from high angular  
428 resolution observations toward the HL TAU region. *The Astrophysical Journal Letters* **808**,  
429 L3 (2015).
- 430 2 Morbidelli, A., Lunine, J. I., O'Brien, D. P., Raymond, S. N. & Walsh, K. J. Building  
431 terrestrial planets. *Annual Review of Earth and Planetary Sciences* **40**, 251-275, d (2012).
- 432 3 Connelly, J. N. *et al.* The Absolute Chronology and Thermal Processing of Solids in the Solar  
433 Protoplanetary Disk. *Science* **338**, 651-655 (2012).
- 434 4 Kruijjer, T. S. *et al.* Protracted core formation and rapid accretion of protoplanets. *Science*  
435 **344**, 1150-1154 (2014).
- 436 5 Pape, J., Mezger, K., Bouvier, A. S. & Baumgartner, L. P. Time and duration of chondrule  
437 formation: Constraints from <sup>26</sup>Al-<sup>26</sup>Mg ages of individual chondrules. *Geochimica et*  
438 *Cosmochimica Acta* **244**, 416-436 (2019).
- 439 6 Budde, G. *et al.* Molybdenum isotopic evidence for the origin of chondrules and a distinct  
440 genetic heritage of carbonaceous and non-carbonaceous meteorites. *Earth and Planetary*  
441 *Science Letters* **454**, 293-303 (2016).
- 442 7 Van Kooten, E. M. M. E. *et al.* Isotopic evidence for primordial molecular cloud material in  
443 metal-rich carbonaceous chondrites. *Proceedings of the National Academy of Sciences of the*  
444 *United States of America* **113**, 2011-2016 (2016).
- 445 8 Warren, P. H. Stable-isotopic anomalies and the accretionary assemblage of the Earth and  
446 Mars: A subordinate role for carbonaceous chondrites. *Earth and Planetary Science Letters*  
447 **311**, 93-100 (2011).
- 448 9 Kruijjer, T. S., Burkhardt, C., Budde, G. & Kleine, T. Age of Jupiter inferred from the distinct  
449 genetics and formation times of meteorites. *Proceedings of the National Academy of Sciences*  
450 **114**, 6712-6716 (2017).
- 451 10 Zinner, E. in *Treatise on Geochemistry (Second Edition)* (eds Heinrich D. Holland & Karl K.  
452 Turekian) 181-213 (Elsevier, 2014).
- 453 11 Dauphas, N. & Schauble, E. A. in *Annual Review of Earth and Planetary Sciences* Vol. 44  
454 709-783 (2016).
- 455 12 McKeegan, K. D. *et al.* The Oxygen Isotopic Composition of the Sun Inferred from Captured  
456 Solar Wind. *Science* **332**, 1528 (2011).
- 457 13 Nanne, J. A. M., Nimmo, F., Cuzzi, J. N. & Kleine, T. Origin of the non-carbonaceous-  
458 carbonaceous meteorite dichotomy. *Earth and Planetary Science Letters* **511**, 44-54 (2019).
- 459 14 Regelous, M., Elliott, T. & Coath, C. D. Nickel isotope heterogeneity in the early Solar  
460 System. *Earth and Planetary Science Letters* **272**, 330-338 (2008).

- 461 15 Poole, G. M., Rehkämper, M., Coles, B. J., Goldberg, T. & Smith, C. L. Nucleosynthetic  
462 molybdenum isotope anomalies in iron meteorites – new evidence for thermal processing of  
463 solar nebula material. *Earth and Planetary Science Letters* **473**, 215-226 (2017).
- 464 16 Worsham, E. A., Bermingham, K. R. & Walker, R. J. Characterizing cosmochemical  
465 materials with genetic affinities to the Earth: Genetic and chronological diversity within the  
466 IAB iron meteorite complex. *Earth and Planetary Science Letters* **467**, 157-166 (2017).
- 467 17 Burkhardt, C. *et al.* Molybdenum isotope anomalies in meteorites: Constraints on solar nebula  
468 evolution and origin of the Earth. *Earth and Planetary Science Letters* **312**, 390-400 (2011).
- 469 18 Budde, G., Burkhardt, C. & Kleine, T. Molybdenum isotopic evidence for the late accretion  
470 of outer solar system material to Earth. *Nature Astronomy* **3**, 736-741 (2019).
- 471 19 Amelin, Y. *et al.* U-Pb chronology of the Solar System's oldest solids with variable  
472  $^{238}\text{U}/^{235}\text{U}$ . *Earth and Planetary Science Letters* **300**, 343-350 (2010).
- 473 20 Kleine, T. & Wadhwa, M. in *Planetesimals: Early Differentiation and Consequences for*  
474 *Planets Cambridge Planetary Science* (eds Benjamin P. Weiss & Linda T. Elkins-Tanton)  
475 224-245 (Cambridge University Press, 2017).
- 476 21 Hevey, P. J. & Sanders, I. S. A model for planetesimal meltdown by  $^{26}\text{Al}$  and its implications  
477 for meteorite parent bodies. *Meteoritics and Planetary Science* **41**, 95-106 (2006).
- 478 22 Scott, E. R. D. Chemical fractionation in iron meteorites and its interpretation. *Geochimica et*  
479 *Cosmochimica Acta* **36**, 1205-1236 (1972).
- 480 23 Bottke, W. F., Nesvornyy, D., Grimm, R. E., Morbidelli, A. & O'Brien, D. P. Iron meteorites  
481 as remnants of planetesimals formed in the terrestrial planet region. *Nature* **439**, 821-824  
482 (2006).
- 483 24 Bizzarro, M., Baker, J. A., Haack, H. & Lundgaard, K. L. Rapid timescales for accretion and  
484 melting of differentiated planetesimals inferred from  $^{26}\text{Al}$ - $^{26}\text{Mg}$  chronometry. *Astrophysical*  
485 *Journal* **632**, L41-L44 (2005).
- 486 25 Kleine, T., Hans, U., Irving, A. J. & Bourdon, B. Chronology of the angrite parent body and  
487 implications for core formation in protoplanets. *Geochimica et Cosmochimica Acta* **84**, 186-  
488 203 (2012).
- 489 26 Touboul, M., Sprung, P., Aciego, S. M., Bourdon, B. & Kleine, T. Hf-W chronology of the  
490 eucrite parent body. *Geochimica et Cosmochimica Acta* **156**, 106-121 (2015).
- 491 27 Schiller, M., Connelly, J. N., Glad, A. C., Mikouchi, T. & Bizzarro, M. Early accretion of  
492 protoplanets inferred from a reduced inner solar system  $^{26}\text{Al}$  inventory. *Earth and Planetary*  
493 *Science Letters* **420**, 45-54 (2015).
- 494 28 van Kooten, E. M. M. E., Schiller, M. & Bizzarro, M. Magnesium and chromium isotope  
495 evidence for initial melting by radioactive decay of  $^{26}\text{Al}$  and late stage impact-melting of the  
496 ureilite parent body. *Geochimica et Cosmochimica Acta* **208**, 1-23 (2017).
- 497 29 Budde, G., Kruijjer, T. S. & Kleine, T. Hf-W chronology of CR chondrites: Implications for  
498 the timescales of chondrule formation and the distribution of  $^{26}\text{Al}$  in the solar nebula.  
499 *Geochimica et Cosmochimica Acta* **222**, 284-304 (2018).
- 500 30 Kruijjer, T. S., Kleine, T., Fischer-Godde, M., Burkhardt, C. & Wieler, R. Nucleosynthetic W  
501 isotope anomalies and the Hf-W chronometry of Ca-Al-rich inclusions. *Earth and Planetary*  
502 *Science Letters* **403**, 317-327 (2014).
- 503 31 Budde, G., Kruijjer, T. S., Fischer-Gödde, M., Irving, A. J. & Kleine, T. Planetesimal  
504 differentiation revealed by the Hf-W systematics of ureilites. *Earth and Planetary Science*  
505 *Letters* **430**, 316-325 (2015).
- 506 32 *Chondrules: Records of Protoplanetary Disk Processes*. (Cambridge University Press, 2018).

- 507 33 Alexander, C. M. O., Grossman, J. N., Ebel, D. S. & Ciesla, F. J. The formation conditions of  
508 chondrules and chondrites. *Science* **320**, 1617-1619 (2008).
- 509 34 Budde, G., Kleine, T., Kruijer, T. S., Burkhardt, C. & Metzler, K. Tungsten isotopic  
510 constraints on the age and origin of chondrules. *Proceedings of the National Academy of*  
511 *Sciences* **113**, 2886-2891 (2016).
- 512 35 Johnson, B. C., Minton, D. A., Melosh, H. J. & Zuber, M. T. Impact jetting as the origin of  
513 chondrules. *Nature* **517**, 339-341 (2015).
- 514 36 Kita, N. T. & Ushikubo, T. Evolution of protoplanetary disk inferred from  $^{26}\text{Al}$  chronology  
515 of individual chondrules. *Meteoritics & Planetary Science* **47**, 1108-1119 (2012).
- 516 37 Nagashima, K., Krot, A. N. & Komatsu, M.  $^{26}\text{Al}$ - $^{26}\text{Mg}$  systematics in chondrules from Kaba  
517 and Yamato 980145 CV3 carbonaceous chondrites. *Geochimica et Cosmochimica Acta* **201**,  
518 303-319 (2017).
- 519 38 Villeneuve, J., Chaussidon, M. & Libourel, G. Homogeneous Distribution of Al-26 in the  
520 Solar System from the Mg Isotopic Composition of Chondrules. *Science* **325**, 985-988,  
521 (2009).
- 522 39 Schrader, D. L. *et al.* Distribution of  $^{26}\text{Al}$  in the CR chondrite chondrule-forming region of the  
523 protoplanetary disk. *Geochimica et Cosmochimica Acta* **201**, 275-302 (2017).
- 524 40 Amelin, Y. & Krot, A. N. Pb isotopic ages of the Allende chondrules. *Meteoritics &*  
525 *Planetary Science* **42**, 1321-1335 (2007).
- 526 41 Amelin, Y., Krot, A. N., Hutcheon, I. D. & Ulyanov, A. A. Lead isotopic ages of chondrules  
527 and calcium-aluminum-rich inclusions. *Science* **297**, 1678-1683 (2002).
- 528 42 Connelly, J., Amelin, Y., Krot, A. N. & Bizzarro, M. Chronology of the solar system's oldest  
529 solids. *Astrophysical Journal* **675**, L121-L124 (2008).
- 530 43 Connelly, J. N. & Bizzarro, M. Pb-Pb dating of chondrules from CV chondrites by  
531 progressive dissolution. *Chemical Geology* **259**, 143-151 (2009).
- 532 44 Bollard, J., Connelly, J. N. & Bizzarro, M. Pb-Pb dating of individual chondrules from the  
533 CBa chondrite Gujba: Assessment of the impact plume formation model. *Meteoritics &*  
534 *Planetary Science* **50**, 1197-1216 (2015).
- 535 45 Krot, A. N., Amelin, Y., Cassen, P. & Meibom, A. Young chondrules in CB chondrites from  
536 a giant impact in the early solar system. *Nature* **436**, 989-992 (2005).
- 537 46 Johnson, B. C., Walsh, K. J., Minton, D. A., Krot, A. N. & Levison, H. F. Timing of the  
538 formation and migration of giant planets as constrained by CB chondrites. *Science Advances*  
539 **2** (2016).
- 540 47 Bollard, J. *et al.* Early formation of planetary building blocks inferred from Pb isotopic ages  
541 of chondrules. *Science Advances* **3**, e1700407 (2017).
- 542 48 Bollard, J. *et al.* Combined U-corrected Pb-Pb dating and  $^{26}\text{Al}$ - $^{26}\text{Mg}$  systematics of individual  
543 chondrules – Evidence for a reduced initial abundance of  $^{26}\text{Al}$  amongst inner Solar System  
544 chondrules. *Geochimica et Cosmochimica Acta* **260**, 62-83 (2019).
- 545 49 Sugiura, N. & Fujiya, W. Correlated accretion ages and  $\epsilon^{54}\text{Cr}$  of meteorite parent bodies and  
546 the evolution of the solar nebula. *Meteoritics & Planetary Science* **49**, 772-787 (2014).
- 547 50 Doyle, P. M. *et al.* Early aqueous activity on the ordinary and carbonaceous chondrite parent  
548 bodies recorded by fayalite. *Nature Communications* **6** (2015).
- 549 51 Jogo, K. *et al.* Mn–Cr ages and formation conditions of fayalite in CV3 carbonaceous  
550 chondrites: Constraints on the accretion ages of chondritic asteroids. *Geochimica et*  
551 *Cosmochimica Acta* **199**, 58-74 (2017).

- 552 52 Fujiya, W., Sugiura, N., Hotta, H., Ichimura, K. & Sano, Y. Evidence for the late formation of  
553 hydrous asteroids from young meteoritic carbonates. *Nature Communications* **3**, 627 (2012)
- 554 53 Brennecka, G. A., Borg, L. E. & Wadhwa, M. Evidence for supernova injection into the solar  
555 nebula and the decoupling of r-process nucleosynthesis. *Proceedings of the National*  
556 *Academy of Sciences* **110**, 17241-17246 (2013).
- 557 54 Jacobsen, B. *et al.* 26Al-26Mg and 207Pb-206Pb systematics of Allende CAIs: Canonical  
558 solar initial 26Al/27Al ratio reinstated. *Earth and Planetary Science Letters* **272**, 353-364  
559 (2008).
- 560 55 MacPherson, G. J., Kita, N. T., Ushikubo, T., Bullock, E. S. & Davis, A. M. Well-resolved  
561 variations in the formation ages for Ca,Al-rich inclusions in the early Solar System. *Earth*  
562 *and Planetary Science Letters* **331-332**, 43-54,  
563 doi:http://dx.doi.org/10.1016/j.epsl.2012.03.010 (2012).
- 564 56 Burkhardt, C., Dauphas, N., Hans, U., Bourdon, B. & Kleine, T. Elemental and isotopic  
565 variability in Solar System materials by mixing and processing of distinct molecular cloud  
566 reservoirs. *Geochimica et Cosmochimica Acta in revision* (2019).
- 567 57 Desch, S. J., Kalyaan, A. & O'D. Alexander, C. M. The Effect of Jupiter's Formation on the  
568 Distribution of Refractory Elements and Inclusions in Meteorites. *The Astrophysical Journal*  
569 *Supplement Series, Volume 238, Issue 1, article id. 11, 31 pp. (2018)*. **238**, 11,  
570 doi:10.3847/1538-4365/aad95f (2018).
- 571 58 Pignatale, F. C., Charnoz, S., Chaussidon, M. & Jacquet, E. Making the Planetary Material  
572 Diversity during the Early Assembling of the Solar System. *The Astrophysical Journal*  
573 *Letters, Volume 867, Issue 2, article id. L23, 7 pp. (2018)*. **867**, L23, doi:10.3847/2041-  
574 8213/aaeb22 (2018).
- 575 59 Yang, L. & Ciesla, F. J. The effects of disk building on the distributions of refractory  
576 materials in the solar nebula. *Meteoritics and Planetary Science* **47**, 99-119,  
577 doi:10.1111/j.1945-5100.2011.01315.x (2012).
- 578 60 Birnstiel, T., Dullemond, C. P. & Pinilla, P. Lopsided dust rings in transition disks. *A&A* **550**  
579 (2013).
- 580 61 Weidenschilling, S. J. Aerodynamics of solid bodies in the solar nebula. *Monthly Notices of*  
581 *the Royal Astronomical Society* **180**, 57-70, doi:10.1093/mnras/180.2.57 (1977).
- 582 62 Lambrechts, M., Johansen, A. & Morbidelli, A. Separating gas-giant and ice-giant planets by  
583 halting pebble accretion. *Astronomy & Astrophysics* **572**, A35, doi:10.1051/0004-  
584 6361/201423814 (2014).
- 585 63 Morbidelli, A. *et al.* Fossilized condensation lines in the Solar System protoplanetary disk.  
586 *Icarus* **267**, 368-376, doi:10.1016/j.icarus.2015.11.027 (2016).
- 587 64 Weber, P., Benítez-Llambay, P., Gressel, O., Krapp, L. & Pessah, M. E. Characterizing the  
588 Variable Dust Permeability of Planet-induced Gaps. *The Astrophysical Journal* **854** (2018).
- 589 65 Schiller, M., Bizzarro, M. & Fernandes, V. A. Isotopic evolution of the protoplanetary disk  
590 and the building blocks of Earth and the Moon. *Nature* **555**, 507 (2018).
- 591 66 Raymond, S. N. & Izidoro, A. Origin of water in the inner Solar System: Planetesimals  
592 scattered inward during Jupiter and Saturn's rapid gas accretion. *Icarus* **297**, 134-148, (2017).
- 593 67 Walsh, K. J., Morbidelli, A., Raymond, S. N., O'Brien, D. P. & Mandell, A. M. A low mass  
594 for Mars from Jupiter's early gas-driven migration. *Nature* **475**, 206-209 (2011).
- 595 68 Pollack, J. B. *et al.* Formation of the Giant Planets by Concurrent Accretion of Solids and  
596 Gas. *Icarus* **124**, 62-85 (1996).
- 597 69 Crida, A., Morbidelli, A. & Masset, F. On the width and shape of gaps in protoplanetary  
598 disks. *Icarus, Volume 181, Issue 2, p. 587-604*. **181**, 587-604, (2006).

599 70 Lambrechts, M. & Johansen, A. Forming the cores of giant planets from the radial pebble flux  
600 in protoplanetary discs. *Astronomy & Astrophysics* **572**, A107 (2014).

601 71 Levison, H. F., Kretke, K. A. & Duncan, M. J. Growing the gas-giant planets by the gradual  
602 accumulation of pebbles. *Nature* **524**, 322-324 (2015).

603 72 Sarafian, A. R. *et al.* Angrite meteorites record the onset and flux of water to the inner solar  
604 system. *Geochimica et Cosmochimica Acta* **212**, 156-166 (2017).

605 73 Sarafian, A. R., Nielsen, S. G., Marschall, H. R., McCubbin, F. M. & Monteleone, B. D.  
606 Early accretion of water in the inner solar system from a carbonaceous chondrite-like source.  
607 *Science* **346**, 623 (2014).

608 74 Amelin, Y. U-Pb ages of angrites. *Geochimica et Cosmochimica Acta* **72**, 221-232 (2008).

609 75 Wang, H. *et al.* Lifetime of the solar nebula constrained by meteorite paleomagnetism.  
610 *Science* **355**, 623 (2017).

611 76 Alibert, Y. *et al.* The formation of Jupiter by hybrid pebble-planetesimal accretion. *Nature*  
612 *Astronomy* (2018).

613 77 Fischer, R. A., Nimmo, F. & O'Brien, D. P. Radial mixing and Ru-Mo isotope systematics  
614 under different accretion scenarios. *Earth and Planetary Science Letters, Volume 482, p. 105-*  
615 *114*. **482**, 105-114 (2018).

616 78 Dauphas, N. The isotopic nature of the Earth's accreting material through time. *Nature* **541**,  
617 521-524 (2017).

618 79 Canup, R. M. & Asphaug, E. Origin of the Moon in a giant impact near the end of the Earth's  
619 formation. *Nature* **412**, 708-712 (2001).

620 80 Alexander, C. M. O. D. *et al.* The provenances of asteroids, and their contributions to the  
621 volatile inventories of the terrestrial planets. *Science* **337**, 721-723 (2012).

622 81 Marty, B. The origins and concentrations of water, carbon, nitrogen and noble gases on Earth.  
623 *Earth and Planetary Science Letters* **313-314**, 56-66 (2012).

624 82 Nesvorný, D., Vokrouhlický, D., Bottke, W. F. & Levison, H. F. Evidence for very early  
625 migration of the Solar System planets from the Patroclus-Menoetius binary Jupiter Trojan.  
626 *Nature Astronomy* **2**, 878-882 (2018).

627 83 Kleine, T. *et al.* Hf-W chronology of the accretion and early evolution of asteroids and  
628 terrestrial planets. *Geochimica et Cosmochimica Acta* **73**, 5150-5188 (2009).

629 84 Kleine, T. & Walker, R. J. Tungsten Isotopes in Planets. *Annual Review of Earth and*  
630 *Planetary Sciences* **45**, 389-417 (2017).

631 85 Rudge, J. F., Kleine, T. & Bourdon, B. Broad bounds on Earth's accretion and core formation  
632 constrained by geochemical models. *Nature Geoscience* **3**, 439-443 (2010).

633 86 Deguen, R., Landeau, M. & Olson, P. Turbulent metal-silicate mixing, fragmentation, and  
634 equilibration in magma oceans. *Earth Planet. Sci. Lett.* **391**, 274-287 (2014).

635 87 Dauphas, N. & Pourmand, A. Hf-W-Th evidence for rapid growth of Mars and its status as a  
636 planetary embryo. *Nature* **473**, 489-492(2011).

637 88 Nimmo, F. & Kleine, T. How rapidly did Mars accrete? Uncertainties in the Hf-W timing of  
638 core formation. *Icarus* **191**, 497-504 (2007).

639 89 Brasser, R., Dauphas, N. & Mojzsis, S. J. Jupiter's Influence on the Building Blocks of Mars  
640 and Earth. *Geophysical Research Letters, Volume 45, Issue 12, pp. 5908-5917* **45**, 5908-5917  
641 (2018).

642 90 Brennecka, G. A. *et al.*  $^{238}\text{U}/^{235}\text{U}$  variations in meteorites: extant  $^{247}\text{Cm}$  and implications for  
643 Pb-Pb dating. *Science* **327**, 449-451 (2010).

644 91 MacPherson, G. J. in *Treatise on Geochemistry* (eds Heinrich D. Holland & Karl K.  
645 Turekian) 1-47 (Pergamon, 2007).

646 92 Burkhardt, C. *et al.* Hf-W mineral isochron for Ca,Al-rich inclusions: Age of the solar system  
647 and the timing of core formation in planetesimals. *Geochimica et Cosmochimica Acta* **72**,  
648 6177-6197 (2008).

649 93 Kööp, L. *et al.* A link between oxygen, calcium and titanium isotopes in <sup>26</sup>Al-poor hibonite-  
650 rich CAIs from Murchison and implications for the heterogeneity of dust reservoirs in the  
651 solar nebula. *Geochimica et Cosmochimica Acta* **189**, 70-95 (2016).

652 94 Sahijpal, S. & Goswami, J. N. Refractory Phases in Primitive Meteorites Devoid of <sup>26</sup>Al  
653 and <sup>41</sup>Ca: Representative Samples of First Solar System Solids? *The Astrophysical Journal*  
654 **509**, L137-L140 (1998).

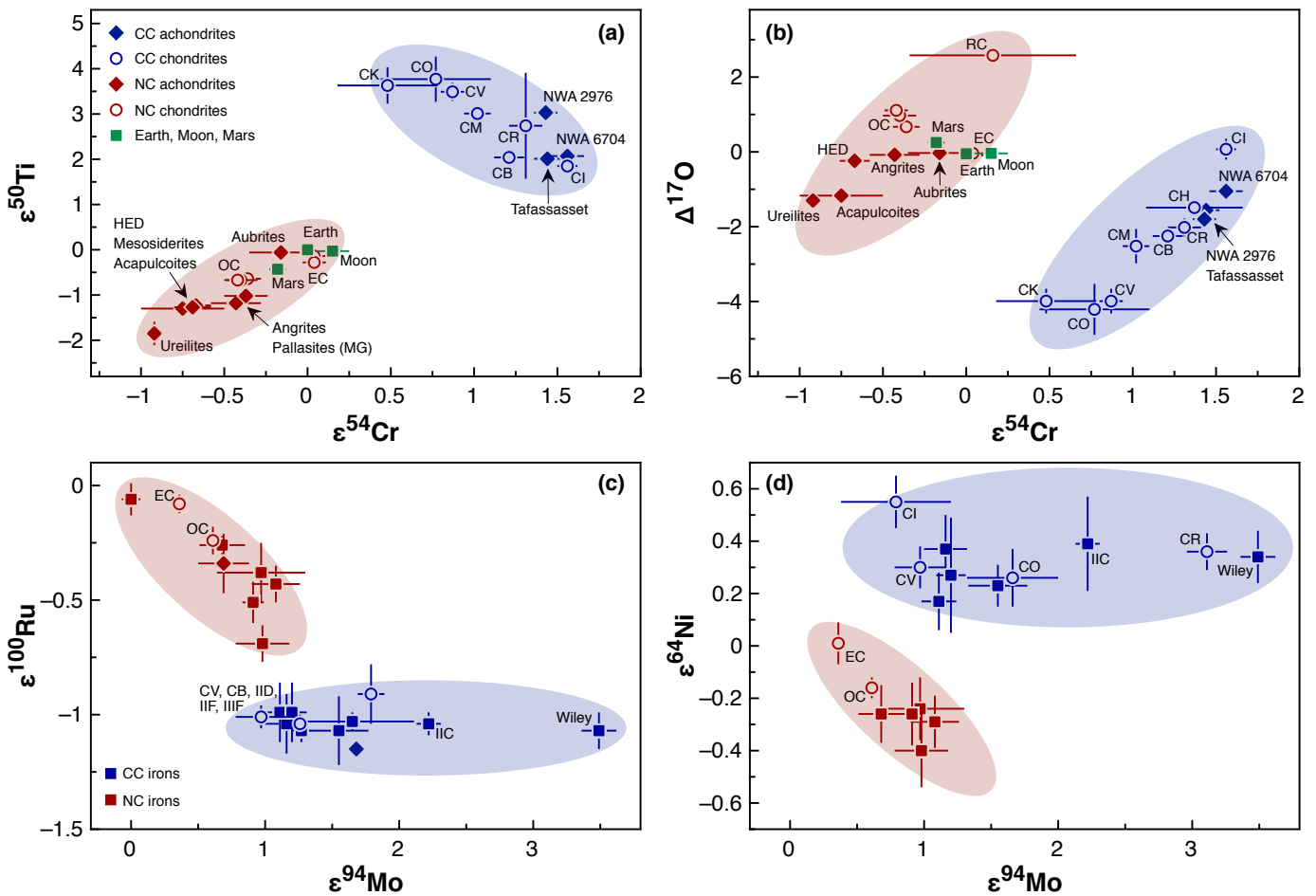
655 95 Wood, J. A. Meteoritic Evidence for the Infall of Large Interstellar Dust Aggregates during  
656 the Formation of the Solar System. *The Astrophysical Journal* **503**, L101-L104 (1998).

657

658

659



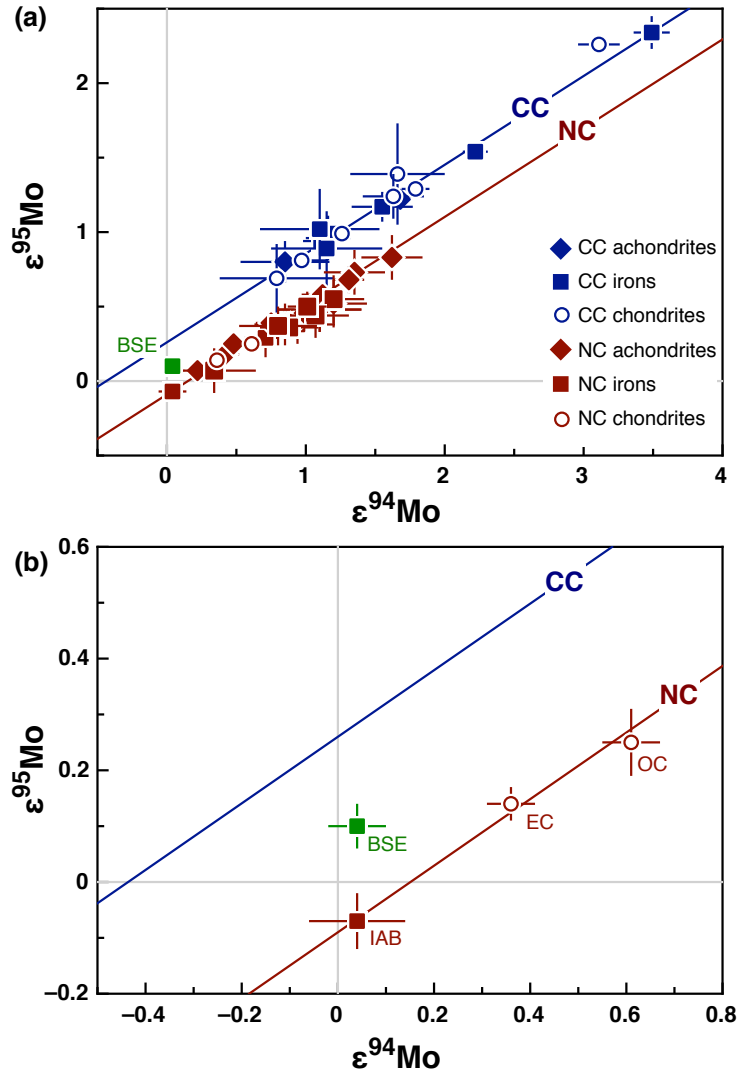


661

662 **Fig. 1: NC-CC meteorite dichotomy inferred from isotopic signatures of bulk meteorites.** (a)  
 663  $\epsilon^{50}\text{Ti}$  vs.  $\epsilon^{54}\text{Cr}$ , (b)  $\Delta^{17}\text{O}$  vs.  $\epsilon^{54}\text{Cr}$ , (c)  $\epsilon^{100}\text{Ru}$  vs.  $\epsilon^{94}\text{Mo}$ , (d)  $\epsilon^{64}\text{Ni}$  vs.  $\epsilon^{94}\text{Mo}$ . Note that 1  $\epsilon$ -unit  
 664 represents the 0.01% deviation (and 1  $\delta$ -unit the 0.1% deviation) in the isotopic ratio of a sample  
 665 relative to terrestrial rock standards. Mass-independent O isotope variations are expressed in  $\Delta^{17}\text{O}$   
 666 ( $\Delta^{17}\text{O} \equiv \delta^{17}\text{O} - 0.52 \delta^{18}\text{O}$ , where 0.52 is the slope of mass-dependent mass fractionation). Note that  
 667  $\Delta^{17}\text{O}$  variations are not nucleosynthetic in origin, but probably reflect photochemical processes in the  
 668 molecular cloud or the solar nebula<sup>12</sup>. Errors bars denote external uncertainties ( $2\sigma$ ) reported in  
 669 respective studies. The isotopic data plotted here are summarized and tabulated in Ref. 18,56.

670

671



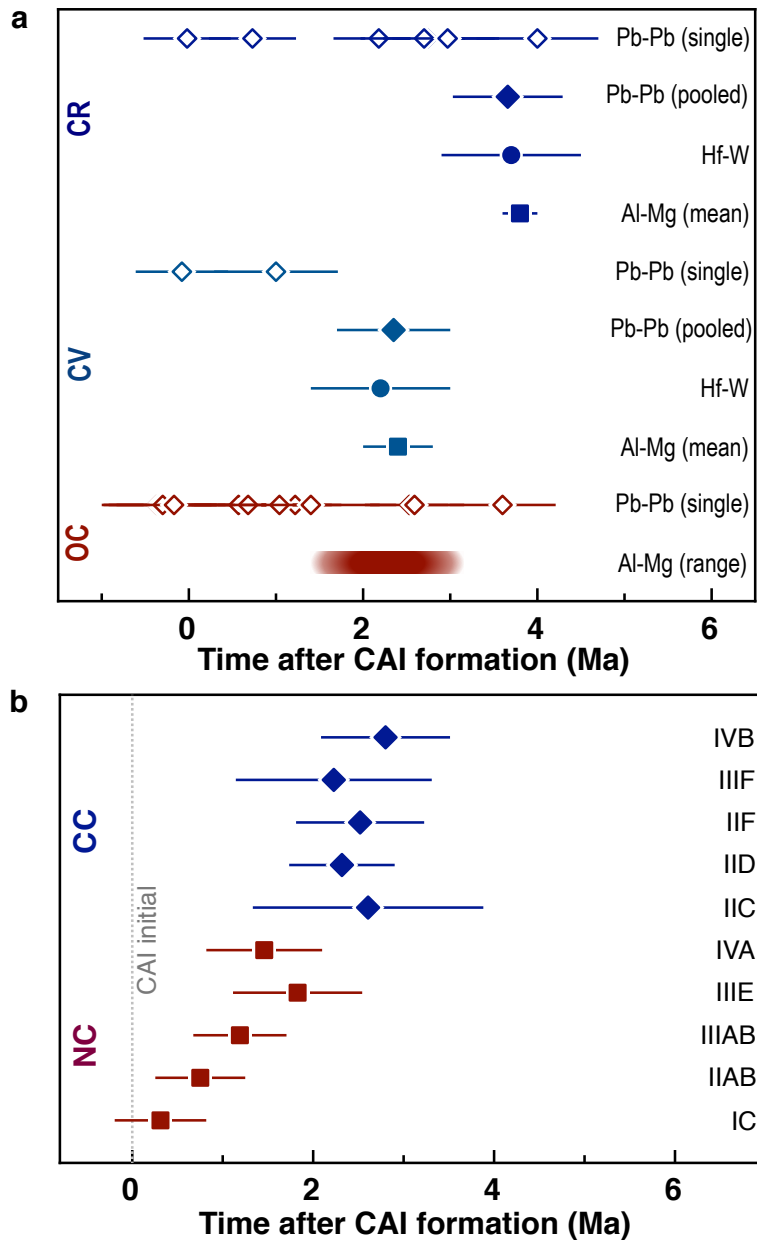
672

673 **Fig. 2: Molybdenum isotope dichotomy of meteorites.** (a)  $\epsilon^{95}\text{Mo}$  vs.  $\epsilon^{94}\text{Mo}$  data for bulk meteorites.  
 674 NC (red) and CC (blue) meteorites define two parallel *s*-process mixing lines with identical slopes,  
 675 but distinct intercept values<sup>6,9,18</sup>. The offset between the two lines reflects an approximately uniform *r*-  
 676 process excess in the CC reservoir relative to the NC reservoir. (b) Zoomed-in version of Fig. 2a  
 677 illustrating that the BSE plots between the NC- and CC-lines. Figure adopted from Budde et al.  
 678 (Ref.18) and plotted NC and CC lines are based on regression results reported in that study. Error bars  
 679 denote external uncertainties reported in respective studies ( $2\sigma$ ). A summary of the Mo isotopic data  
 680 shown in the figure is also given in Ref.18.

681

682

683

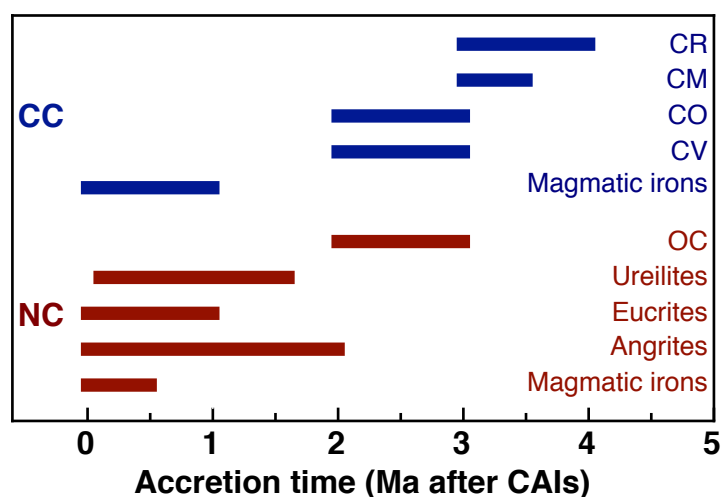


684

685

686 **Fig. 3: Summary of isotopic ages discussed in the text, shown as age intervals relative to CAI**  
 687 **formation.** (a) Pb-Pb, Al-Mg, and Hf-W ages of chondrules. Distinguished are Pb-Pb of single  
 688 chondrules (open symbols; Refs. <sup>3,44</sup>) and pooled chondrule separates (closed symbols; Refs. 40-43),  
 689 Al-Mg ages of ordinary chondrite (OC) chondrules, CV chondrules, and CR chondrules (Refs. 5,36-  
 690 39), and Hf-W ages of CV and CR chondrules (Refs. 29,34). Note that absolute Pb-Pb ages were  
 691 recalculated to age intervals for easy comparison, and all Pb-Pb ages shown are corrected for U isotope  
 692 variability<sup>90</sup>. (b) Core formation of magmatic iron meteorites based on Hf-W chronometry<sup>4,9</sup>.  
 693 Distinguished are NC (IC, IIAB, IIIAB, IIIE, IVA) and CC iron meteorite groups (IIC, IID, IIF, IIIF,  
 694 IVB). Ages for CAIs and Solar System initial values are from Refs. 3,19,30,54.

695



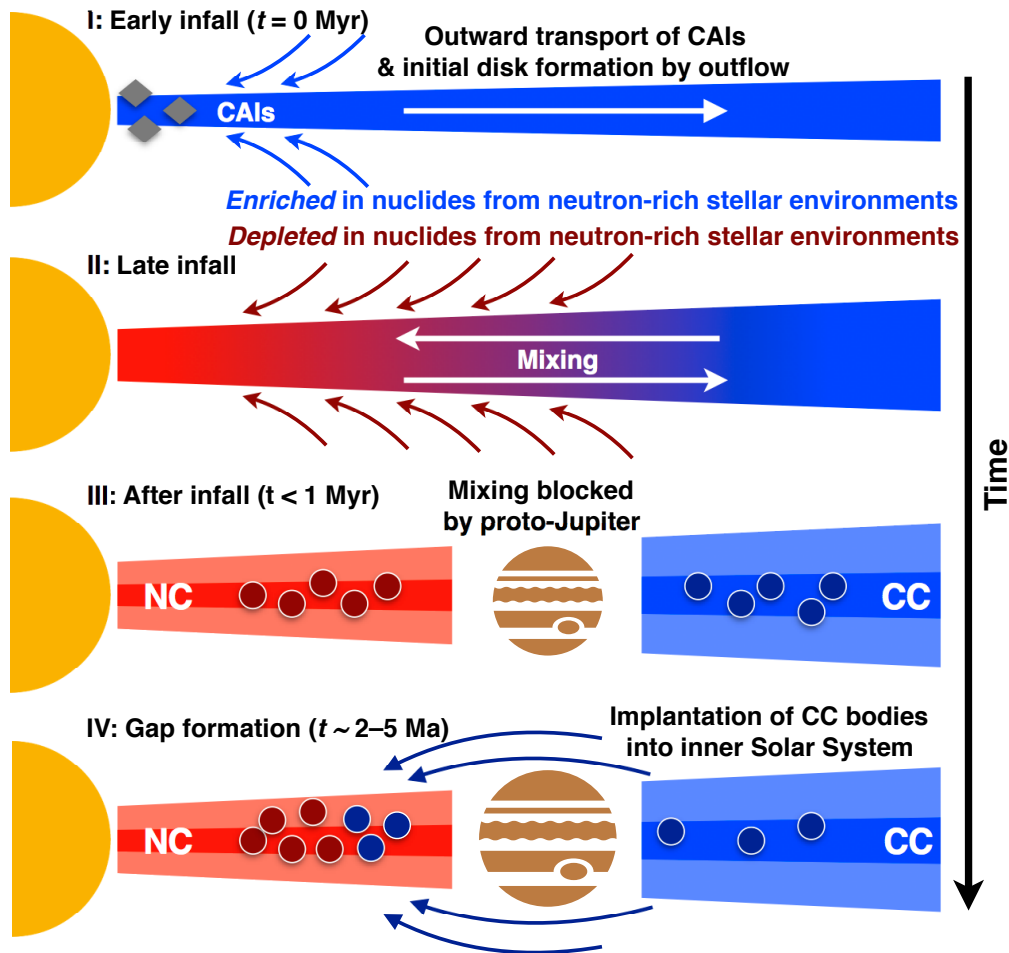
697

698 **Fig. 4: Accretion timescales of meteorite parent bodies as inferred from isotopic ages of**  
 699 **meteorites.** Accretion ages of iron meteorite, angrite, and eucrite parent bodies are inferred from model  
 700 ages for differentiation combined with thermal modelling for internal heating of the parent bodies by  
 701  $^{26}\text{Al}$  decay (see text). Accretion timescales for chondrite parent bodies are based on Al-Mg, Hf-W, and  
 702 Pb-Pb ages obtained for chondrules, and on the chronology of alteration products combined with  
 703 thermal modelling (see text). Note that the horizontal bars reflect the uncertainty of the accretion age  
 704 estimates, and not the duration of accretion.

705

706

707



708 **Fig. 5: Evolution of the solar accretion disk.** Rapid expansion of early infalling material (I) by viscous  
 709 spreading produces an initial disk, whose isotopic composition may be recorded in CAIs. Later infalling  
 710 material (II) was likely more depleted in neutron-rich isotopes (i.e., NC-like). Mixing within the disk  
 711 likely reduced the initial isotopic difference between solids from the inner and outer disk. The  
 712 subsequent rapid formation of Jupiter's core (III) likely prevented exchange and mixing of disk  
 713 materials, thereby maintaining an isotopic difference between the NC and CC reservoirs. Finally (IV)  
 714 the further growth of Jupiter resulted in the formation of a gap within the disk. This coincided with  
 715 scattering of CC bodies from the outer disk into the main asteroid belt<sup>66</sup>, either through Jupiter's growth  
 716 on a fixed orbit and/or by inward migration of Jupiter<sup>67</sup>. Figure adopted and slightly modified from  
 717 Nanne et al.<sup>13</sup>.